JACS
JOURNAL OF THE AMERICAN CHEMICAL SOCIETY
Article
pubs.acs.org/JACS

Symmetry Breaking in the Supramolecular Gels of an Achiral Gelator Exclusively Driven by $\pi-\pi$ Stacking

Zhaocun Shen,[†] Yuqian Jiang,[‡] Tianyu Wang,*[,†] and Minghua Liu*[,†,‡,§]

[†]Beijing National Laboratory for Molecular Science, CAS Key Laboratory of Colloid, Interface and Chemical Thermodynamics, Institute of Chemistry, Chinese Academy of Sciences, Beijing 100190, P. R. China

[‡]National Center for Nanoscience and Technology, Beijing 100190, P. R. China

[§]Collaborative Innovation Center of Chemical Science and Engineering, Tianjin 300072, P. R. China

Supporting Information

ABSTRACT: Supramolecular symmetry breaking, in which chiral assemblies with imbalanced right- and left-handedness emerge from achiral molecular building blocks, has been achieved in the organogels of a C_3-symmetric molecule only via $\pi-\pi$ stacking. Specifically, an achiral C_3-symmetric benzene-1,3,5-tricarboxylate substituted with methyl cinnamate through ester bond was found to form organogels in various organic solvents. More interestingly, when gels formed in cyclohexane, symmetry breaking occurred; i.e., optically active organogels together with the helical nanofibers with predominant handedness were obtained. Furthermore, the stochastically appeared imbalanced helicity could be driven to desired handedness by utilizing slight chiral solvents such as (*R*)- or (*S*)-terpinen-4-ol. Remarkably, the handedness of supramolecular assemblies thus formed could be kept even when the chiral solvents were removed. For the first time, we show that symmetry breaking can occur in supramolecular gel system driven exclusively through $\pi-\pi$ stacking.

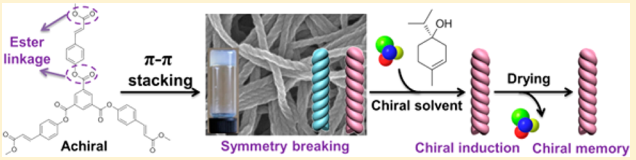

INTRODUCTION

Although it remains a mystery for the origin of homochirality in nature,[1] many researchers do have found that achiral or dynamically racemic molecules could generate optical activity with symmetry breaking. This situation has been found in crystals,[2] liquid crystals,[3] self-assembled molecular systems such as aggregates,[4] and supramolecular gels.[5] Such a phenomenon is also found in the confined systems such as micelles[6] and Langmuir or Langmuir–Blodgett (LB) films[7] organized through the air/water interfacial assembly, which adds much knowledge to the better understanding of the origin of chirality in nature. In the confined systems such as LB films, many molecules can show symmetry breaking phenomenon, where unilateral compression plays an important role. However, in the self-assembled solution, gels, or liquid crystals, only limited molecules have such properties. Moreover, in these molecular systems such as tetraphenylporphyrin sulfonate (TPPS), organic dyes, and other related molecules, combined non-covalent interactions including hydrogen bonding, electrostatic interaction, and $\pi-\pi$ stacking are generally necessary. For example, in the case of TPPS aggregates,[4b] both the hydrogen bonding and electrostatic interaction played important roles. In the other case, Meijer and co-workers have found that the symmetry breaking occurs in the self-assembled achiral partially fluorinated benzene-1,3,5-tricarboxamides in solution, where the 3-fold hydrogen bonding and dipole–dipole interaction play important roles.[4i] In supramolecular gel system, we have also found that the self-assembly of an achiral C_3-symmetric benzene-1,3,5-tricarboxamide substituted with ethyl cinnamate can form assemblies with macroscopic chirality, in which hydrogen bonding and $\pi-\pi$ interaction play very important roles.[5c] Unfortunately, for supramolecular assemblies in solution or gel systems, symmetry breaking is never driven exclusively by weak $\pi-\pi$ interaction.

In a series of work on the C_3-symmetric π-gel research, we have designed four achiral C_3-symmetric molecules, which have three π-conjugated cinnamate substituents connected to the benzene ring via ester linkage rather than amide groups (Scheme 1). These molecules have methyl ester (BTECM), ethyl ester (BTECE), *n*-propyl ester (BTECP), or *n*-butyl ester (BTECB) end chains. We have unexpectedly found that only BTECM could form supramolecular gels in different solvents, while the other three molecules could not gelate any solvents. Remarkably, although BTECM was achiral, it could form chiral supramolecular gels in cyclohexane with symmetry breaking. The supramolecular chirality of the gels could be proved by both optical activity and chiral nanostructures. Since there is no any other noncovalent interactions except for $\pi-\pi$ stacking, we have discovered that purely $\pi-\pi$ stacking can also drive the symmetry breaking in the supramolecular gel system.

On the other hand, for the symmetry breaking system, the control of the handedness is very important. Although the vortex force[4e,f,8] and magnetic force[4h] have been proved to be effective, the addition of the chiral substance through the sergeant and soldier rule[9] is quite usual. We have found that through addition of a small amount of chiral solvents the symmetry breaking could be controlled. More interestingly,

Received: October 7, 2015
Published: December 8, 2015

DOI: 10.1021/jacs.5b10496
J. Am. Chem. Soc. 2015, 137, 16109–16115

Scheme 1. Molecular Structure of the Achiral C_3-Symmetric Derivatives and Schematic Illustration of Symmetry Breaking in Cyclohexane Purely through $\pi-\pi$ Stacking and Supramolecular Chirality Memory with the "Add–Remove Chiral Solvents" Procedure

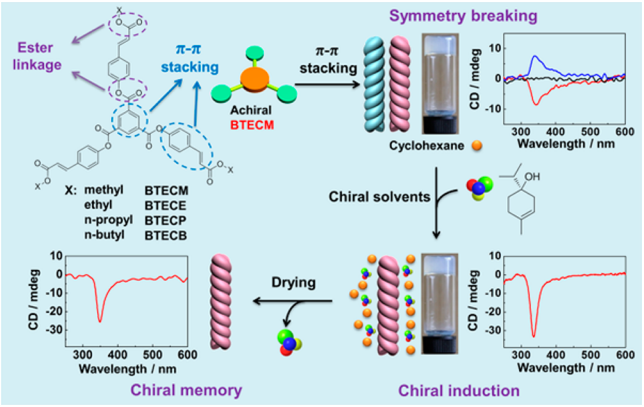

when the chiral solvents were removed, the chirality could be maintained. By using an "add–remove chiral solvents" procedure, the handedness of BTECM assemblies could be easily controlled without damaging the purity of these supramolecular gels (Scheme 1). Thus, constructing chiral supramolecular gels from the symmetry breaking of achiral molecules purely via $\pi-\pi$ interaction and controlling their handedness by chiral solvents with chiral memory have been established.

RESULTS AND DISCUSSION

Self-Assembly of Achiral C_3-Symmetric Molecules in Various Solvents. The achiral C_3-symmetric molecules had three rigid π-conjugated cinnamate substituents connecting to the benzene ring core with only ester groups. On the edges of these achiral molecules, different alkyl esters groups were introduced, as shown in Scheme 1. These molecules could disperse in many organic solvents. Upon heating, BTECM could form transparent solution in both nonpolar solvents (toluene and cyclohexane) and polar solvents (methanol and ethanol), which then changed into supramolecular gels after cooling down to the room temperature (Table 1). For all the BTECM gels, the temperature responsive sol–gel transitions were fully reversible (Figure S1). In cyclohexane, BTECM could be supergelator with very low critical gelation concentration (0.1% w/v). Interestingly, although BTECE had a similar molecular structure to BTECM, it could not form supramolecular gels in any solvents (Table 1). Furthermore, the molecules containing longer end chains (BTECP and BTECB) also could not form gels (Table 1).

The self-assembled nanostructures from BTECM gels were studied by scanning electron microscopy (SEM) measurements (Figure 1). The results showed that BTECM self-assembled into one-dimensional nanostructures, such as nanofibers and nanoribbons, depending on the solvents. It was worth mentioning that these self-assembled one-dimensional nanostructures were relatively thick in methanol and could be very thin in cyclohexane. BTECE formed precipitates instead of gels, and the morphologies of BTECE precipitates in ethanol, methanol, and cyclohexane were also investigated by SEM, as shown in Figure 1. In polar solvents like ethanol or methanol, BTECE self-assembled into spherical structures (Figure 1b,d).

Table 1. Gelation Properties of BTECM, BTECE, BTECP, and BTECB in Various Solvents[a]

solvent	BTECM	BTECE	BTECP	BTECB
H_2O	I	I	I	I
acetonitrile	S	S	S	S
methanol	G	P	P	P
ethanol	G	P	P	P
acetone	P	S	S	S
dioxane	S	S	S	S
$CHCl_3$	S	S	S	S
ethyl acetate	P	P	S	S
CH_2Cl_2	S	S	S	S
toluene	G	S	S	S
cyclohexane	G	P	P	P
n-hexane	I	P	P	P
THF	S	S	S	S
DMF	S	S	S	S
DMSO	S	S	S	S

[a]G: stable gel; S: soluble; I: insoluble; P: precipitate.

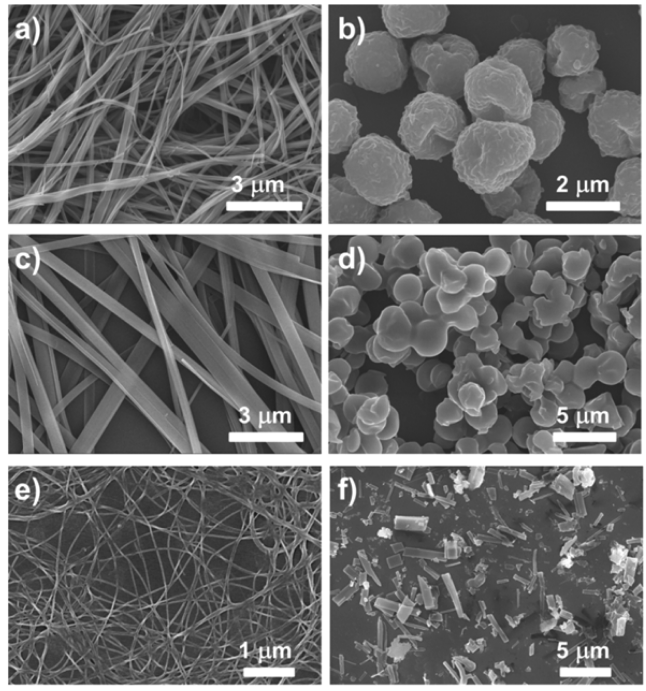

Figure 1. SEM images of the BTECM gels (0.3% w/v) and BTECE precipitates (0.3% w/v) in various solvents: (a) BTECM in ethanol, (b) BTECE in ethanol, (c) BTECM in methanol, (d) BTECE in methanol, (e) BTECM in cyclohexane, and (f) BTECE in cyclohexane.

However, for the BTECE assemblies in cyclohexane, only disordered morphologies could be observed (Figure 1f). Considering the fact that the structural difference between BTECE and BTECM was only one methylene group, these different self-assembled morphologies and gelation properties were remarkable. Presumably, the steric hindrance from the ethyl ester end chain played an important role. Although BTECP and BTECB also could not form gels, their nanostructures were studied by SEM measurements (Figure S2). The results showed that these molecules always self-assembled into very huge ribbon or rodlike morphologies.

DOI: 10.1021/jacs.5b10496
J. Am. Chem. Soc. 2015, 137, 16109–16115

Chiral Helices from Symmetry Breaking of Achiral BTECM. More interestingly, the enlarged SEM image of BTECM gels in cyclohexane showed very nice left- (*M*) and right-handed (*P*) uniform helical fibers with the diameter about 50 nm (Figure 2a). Additionally, the circular dichroism (CD)

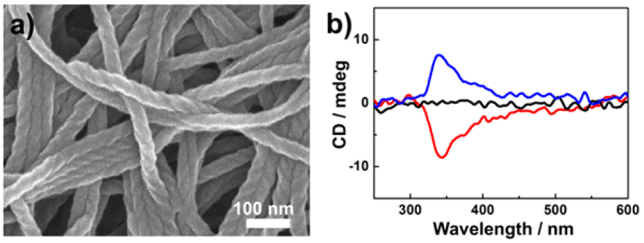

Figure 2. SEM image (a) and CD spectra (b) of the translucent BTECM gels (0.2% w/v) in cyclohexane. For the CD spectra, gels from different batches showed different CD signs due to symmetry breaking.

spectra of these BTECM assemblies showed a positive or negative Cotton effect at 340 nm (Figure 2b), even though BTECM was an achiral molecule. Furthermore, the authenticity of the circular dichroism was confirmed by the negligible linear dichroism (LD) artifacts in the system (Figure S3a). This result indicated that symmetry breaking could occur in the cyclohexane gels of BTECM. The statistical distribution of the handedness and intensity of the CD signals from 30 samples of BTECM gels in cyclohexane was analyzed (Figure S3b). The results showed that the supramolecular chirality obtained from the assembly of achiral molecules was random.[10] Moreover, the distribution of optical activity from totally 30 samples was Gaussian-like (Figure S3c).[2b] Although BTECM could also form supramolecular gels in methanol, ethanol, and toluene, no helical nanostructures and optical activity were detected from these assemblies. The symmetry breaking within BTECM assemblies could only happen in cyclohexane. In contrast, BTECE, BTECP, and BTECB could neither form the gels nor show the chiral structures.

$\pi-\pi$ Interaction as Driving Force for Gelation and Symmetry Breaking. In order to further investigate the gelation mechanism of BTECM and symmetry breaking in cyclohexane, UV−vis spectra, fluorescence spectra, X-ray diffraction (XRD) pattern, and temperature-dependent ^{1}H NMR spectra of BTECM assemblies were measured. Figure 3a showed the UV−vis spectra of the gels in comparison with that in solution. The diluted BTECM cyclohexane solution (0.1 mmol L^{-1}) showed a sharp absorption band at 282 nm, while the BTECM gels in cyclohexane exhibited a red-shift of the absorption band, indicating the J-aggregation of π-conjugated substituents within assemblies.[11] The fluorescence spectra of BTECM solution and gels were also studied. The strong fluorescence enhancement after gelation could be detected (Figure S4). These results all supported the close packing of π-conjugated systems via $\pi-\pi$ interaction within the helical fibers,[12] which were formed upon BTECM gelation in cyclohexane.

The XRD pattern of BTECM gels in cyclohexane clearly suggested the $\pi-\pi$ stacking and columnar aggregates, as shown in Figure 3b. Specifically, the XRD diffraction peaks with 2θ values at 4.96, 6.98, 9.87, 10.87, 16.57, and 18.69 fully matched the ratio of $1:\sqrt{2}:2:\sqrt{5}:\sqrt{11}:\sqrt{14}$, indicating the formation of a rectangular columnar aggregate in the helical fibers with

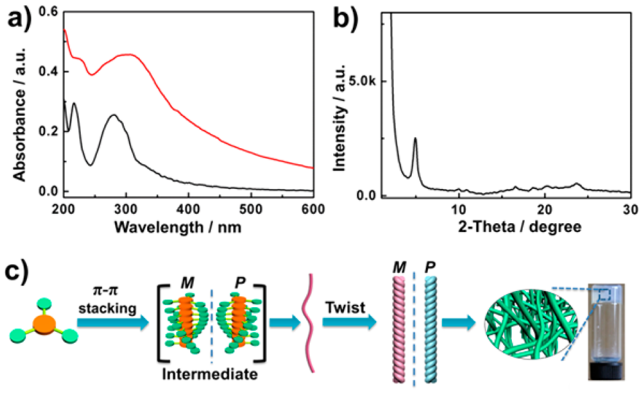

Figure 3. (a) UV−vis spectra of BTECM gels (0.2% w/v, red curve) and solution in cyclohexane (0.1 mmol L^{-1}, black curve). (b) XRD pattern of BTECM gels (0.2% w/v) in cyclohexane. (c) The possible mechanism of BTECM gelation in cyclohexane.

diameter of columnar aggregate 1.78 nm.[13] In addition, a broad diffraction peak with 2θ value of 23.84 corresponded to the *d*-spacing of 0.37 nm, which suggested the $\pi-\pi$ stacking between π-conjugated substituents within BTECM assemblies. The $\pi-\pi$ stacking could also be clearly proved by temperature-dependent ^{1}H NMR measurements. When the temperature was decreased from 95 to 25 °C, BTECM could form compacted assemblies. In this case, the changes of the corresponding ^{1}H NMR spectra were followed, as shown in Figure S5. The signals of all the aromatic protons showed downfield shift upon decreasing the temperature. These results strongly suggested that every aromatic rings of BTECM were involved into the $\pi-\pi$ interaction during the self-assembly.

For the gelation and symmetry breaking of BTECM assemblies in cyclohexane, the $\pi-\pi$ interaction plays a very important role, which has been demonstrated by a variety of spectroscopic measurements, as described above. On the other hand, overcrowded molecular packing is necessary for the symmetry breaking within supramolecular assemblies. For BTECM gels with supramolecular chirality, the overcrowded molecular packing has been constructed by $\pi-\pi$ interaction. Comparing with the hydrogen bonding, the $\pi-\pi$ interaction can be relatively weak. Therefore, the larger ethyl group at the edge of BTECE molecules could interfere the $\pi-\pi$ stacking, and BTECE could not form chiral assemblies and gels. Similarly, the steric hindrance could also come from the longer end chains of BTECP and BTECB. However, for BTECM, the $\pi-\pi$ interaction between different benzene rings and cinnamate substituents were still strong enough to make BTECM assemble into chiral helical fibers. Thus, the aggregation of BTECM could initially generate *P* or *M* conformer by chance, and those small helical aggregates could grow up to become longer one-dimensional helical aggregates by following the original chiral conformation. Several one-dimensional helical aggregates further twisted into larger helical fibers. At last, those helical fibers intertwined with each other to gelate the solvent (Figure 3c).[14]

Molecular Dynamics Simulation for Symmetry Breaking. For further understanding the effect of substituent groups during self-assembly with symmetry breaking, molecular dynamics (MD) calculations were performed on BTECM and BTECE. Considering the C_3-symmetrical character of BTECM/BTECE, we optimized their molecular structure in C_3-symmetry at B3LYP/6-31G(d,p) level with the Gaussian09

DOI: 10.1021/jacs.5b10496
J. Am. Chem. Soc. 2015, 137, 16109−16115

program.[15] The freely rotating benzenes in side chains led to two equilibrium conformations with equal energies (Figure S6). With optimized molecular geometry, we built columnar aggregates containing 20 molecules with 3.7 Å *d*-spacings for BTECM/BTECE in the MD simulations (Figure S7). We solvated the preassembly aggregates of BTECM/BTECE in the solvent cyclohexane (2800 molecules) with the PACKMOL program.[16] Then MD simulations of the systems were performed within NPT ensemble (constant number of atoms, pressure, and temperature) in GROMACS-4.6.7.[17] A Berendsen thermostat with a time step of 1 fs was employed to regulate the temperature at 298 K. All simulations were carried out for 3 ns to achieve a fully relaxed configuration by using the General Amber Force-Field (GAFF).[18] Both the total energy and density reached a dynamic equilibrium after 200 ps for two systems (Figure S8), and the average density was 0.77 g mL^{-1}, which agreed with that of cyclohexane liquid. We extracted the configurations every 0.1 ps and calculated the average structures for both BTECM and BTECE aggregations after 200 ps of dynamics. The average configurations presented in Figure 4 and

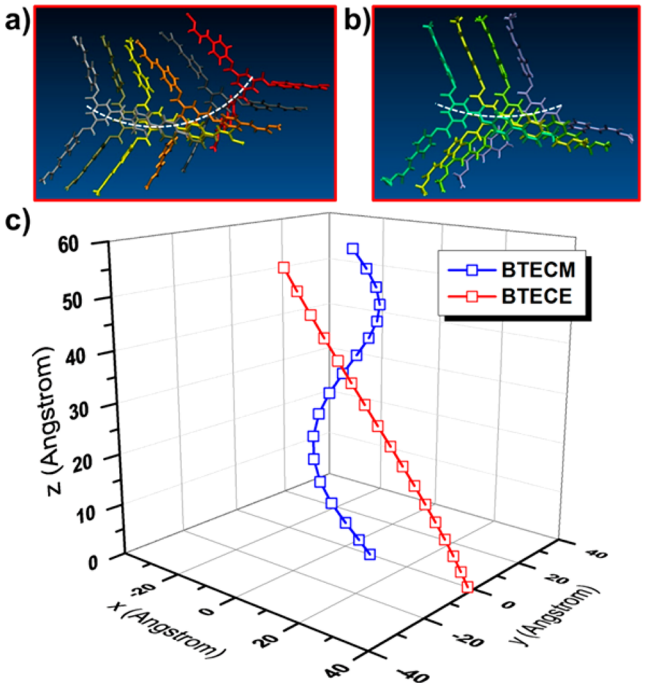

Figure 4. Molecular models illustrating the average configurations in the supramolecular columnar aggregates of BTECM (a) and BTECE (b) after 200 ps of dynamics. (c) The fitted helices of BTECM and BTECE columnar aggregates according to the average configurations.

Figure S9 demonstrated that the helix could exactly be formed for BTECM rather than BTECE in cyclohexane. The cinnamate substituents of BTECM molecules were closer to their neighbors with stronger $\pi-\pi$ interaction, resulting in the formation of a helix. While for BTECE, the steric hindrance of ethyl in the terminal group greatly decreased the $\pi-\pi$ interaction among different cinnamate substituents, so BTECE molecules could not form helical nanostructures.

By assuming both BTECM and BTECE can self-assemble into columnar aggregates, we fitted the helical pitch and radius according to their regular aggregation structures in Figure 4. When the *d*-spacings between BTECM/BTECE molecules were all set as 0.37 nm, the fitted radius and pitch for BTECM helix were 0.83 and 5.34 nm, respectively (Figure 4c). The calculated radius of BTECM helix matched well with the results from XRD measurements. However, for the fitted radius and pitch of BTECE assemblies, 3.83 and 30.4 nm were obtained, respectively (Figure 4c), indicating that BTECE assemblies could not form reasonable helical structures.

Furthermore, we built the models of BTECM single helix and BTECE assemblies, as shown in Figure 5. From the models

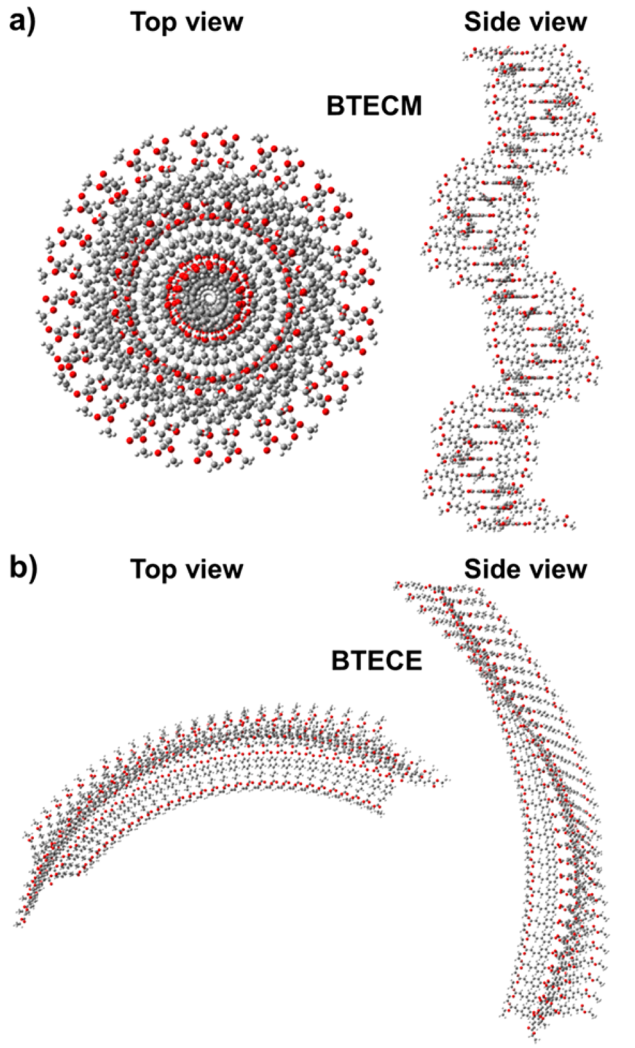

Figure 5. Models of BTECM (a) and BTECE (b) helical columns contained 30 molecules.

simulated by molecular dynamics combined with mathematical method, the difference between BTECM and BTECE could be easily observed. BTECM assemblies were easy to form a beautiful helix, while the assembly of BTECE molecules could hardly form a regular helix. Therefore, the effect of end alkyl chains length on symmetry breaking during self-assembly of achiral C_3-symmetric molecules has been determined by both of the experimental data and theoretical MD simulations.

Determined Handedness of Supramolecular Chiral Assemblies and the Chiral Memory by Trace Chiral Solvents. Although BTECM can self-assemble into supramolecular gels with macroscopic chirality, the handedness of the assemblies is produced by chance. Actually, the chiral supramolecular gels formed by achiral molecules with controllable handedness can be much more useful, especially when

DOI: 10.1021/jacs.5b10496
J. Am. Chem. Soc. 2015, 137, 16109−16115

there are no any chiral dopants remaining in the systems. Because the driving force for forming BTECM assemblies is weak $\pi-\pi$ interaction, the chirality of BTECM gels can be easily changed by physically mixing some chiral organic molecules or solvents.[19] In order to prove the effect of the solely $\pi-\pi$ stacking interaction, we selected two kinds of chiral solvents with $\pi-\pi$ stacking ability.

We tried to add several types of chiral solvents into the BTECM gels in cyclohexane to control the handedness of corresponding supramolecular chirality. These chiral solvents could have either aromatic rings or hydroxyl groups or be just simple alkane with alkene groups (Chart 1). Interestingly, all

Chart 1. Chiral Solvents Used for Controlling the Handedness of Supramolecular Chirality of BTECM Gels

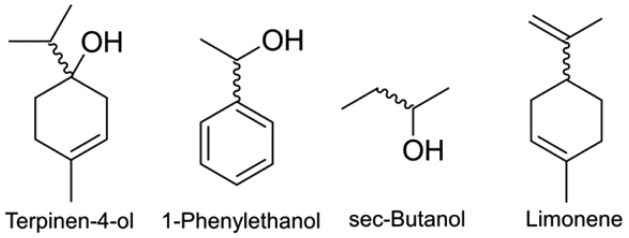

these chiral solvents with low molecular weight could help BTECM self-assemble into chiral gels with determined handedness, as demonstrated by the CD spectral measurements (Figure 6a and Figure S10). For example, for the BTECM gels

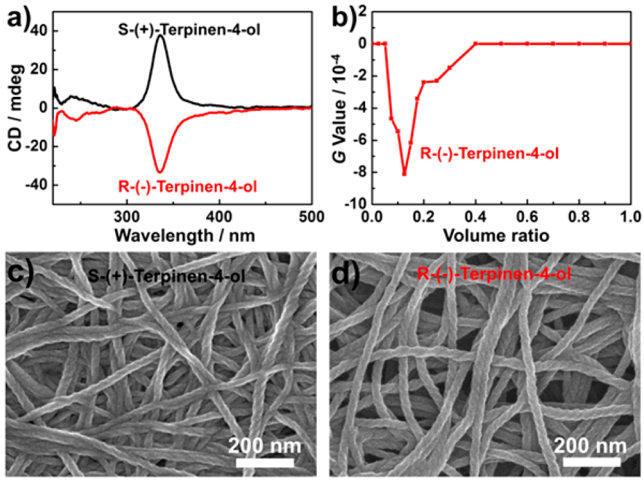

Figure 6. (a) CD spectra of the BTECM gels (0.2% w/v) containing *R*-(−)-terpinen-4-ol (red curve) or *S*-(+)-terpinen-4-ol (black curve) with volume ratio of terpinen-4-ol/(cyclohexane + terpinen-4-ol) equal to 0.125. (b) *G* value of BTECM gels (0.2% w/v) centered at 336 nm as a function of volume ratio of *R*-(−)-terpinen-4-ol/(cyclohexane + *R*-(−)-terpinen-4-ol). (c, d) SEM images of the BTECM gels (0.2% w/v) containing *S*-(+)-terpinen-4-ol (c) or *R*-(−)-terpinen-4-ol (d) with volume ratio of terpinen-4-ol/(cyclohexane + terpinen-4-ol) equal to 0.125.

containing *S*-(+)-terpinen-4-ol and cyclohexane with volume ratio of terpinen-4-ol/(cyclohexane + terpinen-4-ol) equal to 0.125, a strong CD signal with a positive Cotton effect at 336 nm could be detected (Figure 6a). In addition, the SEM image obtained from the same sample showed mainly *P* helical fibers (Figure 4c). In contrast, in the case of BTECM gels containing *R*-(−)-terpinen-4-ol, the mirror-imaged CD spectrum (Figure 6a) and *M* helical fibers could always be observed (Figure 6d).

Moreover, for controlling the handedness of supramolecular chirality within BTECM gels, the volume ratios between chiral solvents and cyclohexane were very important. This issue has been investigated by measuring the *G* value of the CD spectra as well as the SEM of BTECM gels formed in cyclohexane/*R*-(−)-terpinen-4-ol mixture with different volume ratios. Since *G* value is independent of absorption intensity or sample thickness, the quantitative analysis of *G* value can clearly suggest the optical activity of the systems. In general, more chiral *R*-(−)-terpinen-4-ol in the system could produce stronger supramolecular chirality (Figure 6b). However, too much chiral solvent could also destroy the helical fibers (Figure S11) and lead to the disappearance of CD signals (Figure 6b). Although 7.5% chiral *R*-(−)-terpinen-4-ol was good enough to control the handedness of supramolecular chirality of BTECM gels, the sample with volume ratio of terpinen-4-ol/(cyclohexane + terpinen-4-ol) equal to 0.125 gave the maximum *G* value upon the CD spectral measurement.

Particularly, within these chiral supramolecular gels, chiral solvents were included by physically mixing, and the boiling points of these chiral solvents are relatively low. Thus, these chiral solvents can be completely removed from the systems by high vacuum. This issue could be proved by ^{1}H NMR measurements, as shown in Figure S12. No signals of chiral solvents were detected from the ^{1}H NMR spectra of vacuum-dried chiral supramolecular gels. Most importantly, the CD spectra of BTECM xerogels after vacuum-drying also showed obvious Cotton effects similar to the BTECM gels containing chiral solvents, which suggested the "chirality memory" of BTECM gels (Figure 7).[20] Although chirality memory has been

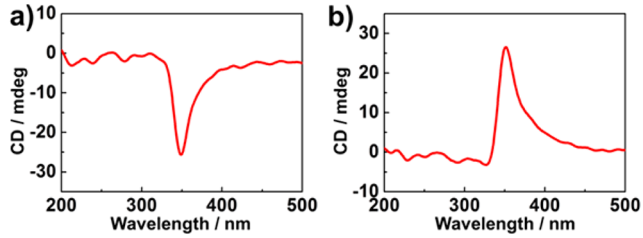

Figure 7. Chiral memory effect demonstrated by the CD spectra of BTECM xerogels with chiral solvents completely removed by high vacuum. Either *R*-(−)-terpinen-4-ol (a) or *S*-(+)-terpinen-4-ol (b) can be used as chiral solvents. The volume ratio of terpinen-4-ol/(cyclohexane + terpinen-4-ol) is equal to 0.125.

achieved in synthetic polymers or other self-assembled systems, to the best of our knowledge, this is the first time achieving "chirality memory" within low-molecular-weight supramolecular gels. Therefore, by using an "add−remove chiral solvents" procedure, the chiral supramolecular gels without any chiral molecules but with controllable handedness have been constructed.

CONCLUSIONS

In conclusion, an achiral C_3-symmetric benzene-1,3,5-tricarboxylate substituted with methyl cinnamate (BTECM) through ester bond was found to form supramolecular gels and further showed symmetry breaking. Since the compound had no hydrogen bonding sites, no long alkyl chains, and no charges, it was demonstrated that symmetry breaking was driven purely by

DOI: 10.1021/jacs.5b10496
J. Am. Chem. Soc. 2015, 137, 16109−16115

the $\pi-\pi$ stacking in the supramolecular gel system. Although the emergence of the macroscopic chirality in the system was by chance, the handedness of the supramolecular assemblies could be further controlled by small amount of chiral solvents. Moreover, upon removing the chiral solvents, the chirality of the assemblies could be memorized. This work provides the solid example that only weak $\pi-\pi$ stacking other than the hydrogen bonding and electrostatic interaction can also lead to the symmetry breaking in the self-assembled system and gives a further understanding of the homochirality in nature.

EXPERIMENTAL SECTION

Materials Preparation. All the starting materials and solvents were obtained from commercial suppliers and used as received. 1,3,5-Benzenetricarbonyl trichloride was purchased from Alfa Aesar. Methyl 4-hydroxycinnamate and ethyl 4-hydroxycinnamate were purchased from TCI and Adamas, respectively. *R*-(−)-Terpinen-4-ol and *S*-(+)-terpinen-4-ol were purchased from TCI. *R*-(+)-1-Phenylethanol and *S*-(−)-1-phenylethanol were purchased from Alfa Aesar. *R*-(+)-Limonene and *S*-(−)-limonene were purchased from TCI. (*R*)-(−)-*sec*-Butanol and (*S*)-(+)-sec-butanol were purchased from TCI. The experimental details for the synthesis of BTECM, BTECE, BTECP, and BTECB are provided in the Supporting Information.

Gels Formation in Organic Solvents. A typical procedure for the gels formation in methanol, ethanol and cyclohexane is as follows: 3 mg of BTECM and 1 mL of solvent were mixed in a sealed tube. The BTECM was dissolved completely upon heating, then the solution was slowly cooled to room temperature, and the gel was obtained after 1 h. Gelation was confirmed by the absence of flow, as observed by the tube inversion method.

Precipitates Formation in Organic Solvents. A typical procedure for the precipitates formation in organic solvents is as follows: 3 mg of BTECM, BTECE, BTECP, or BTECB and 1 mL of solvent were mixed in a sealed tube. The derivative was dissolved completely upon boiling, then the solution was slowly cooled to room temperature, and white precipitates were obtained overnight.

UV−Vis Absorption Spectra. UV−vis spectra were recorded in quartz cuvettes (light path 0.1 mm) on a JASCO UV-550 spectrometer.

Fluorescence Emission Spectra. Fluorescence spectra were recorded in quartz cuvettes (light path 2 mm) on a Hitachi F-4500 fluorescence spectrophotometer. The EX slit and EM slit were set as 5 nm, and the PMT voltage was set as 400 V. Excitation wavelengths are specified in the corresponding figure captions.

Circular Dichroism (CD) Spectra. CD spectra were recorded in quartz cuvettes (light path 0.1 mm) on a JASCO J-810 spectrophotometer. For the study about chiral memory, the samples were prepared as cast films on quartz plates and dried upon high vacuum. For the measurement of the CD spectra, the quartz cuvettes or quartz plates were placed perpendicular to the light path of CD spectrometer and rotated within the quartz cuvettes plane to rule out the possibility of the birefringency phenomena and eliminate the possible angle dependence of the CD signal.

^{1}H NMR Spectra. ^{1}H NMR (400 MHz) spectra were recorded on a Bruker Avance 400 spectrometer with TMS as internal standard at 298 K. Temperature-dependent ^{1}H NMR (300 MHz) spectra were recorded on a Bruker DMX300 spectrometer with TMS as internal standard.

Mass Spectra and Elemental Analysis. Mass spectral data were obtained by using a BIFLEIII matrix-assisted laser desorption/ionization time of fight mass spectrometry (MALDI-TOF MS) instrument. Elemental analysis was performed on a Thermo Flash EA-1112 Series NCHS-O analyzer.

Scanning Electron Microscopy (SEM). SEM images were recorded on a Hitachi S-4800 FE-SEM instrument with an accelerating voltage of 10 kV. Before SEM measurement, the samples on silicon wafers were coated with a thin layer of Pt to increase the contrast.

X-ray Diffraction (XRD). XRD analysis was performed on a Rigaku D/Max-2500 X-ray diffractometer (Japan) with Cu Kα radiation (λ = 1.5406 Å), which was operated at a voltage of 40 kV and a current of 200 mA. Samples were cast on glass substrates and vacuum-dried for XRD measurements.

Handedness Control of Chiral BTECM Gels. A typical procedure for adding chiral solvents into BTECM gels in cyclohexane is as follows: 2 mg of BTECM, x mL of cyclohexane, and $(1-x)$ mL of R/S-terpinen-4-ol were mixed in a sealed tube. The BTECM was dissolved completely upon boiling, then the solution was slowly cooled to room temperature, and the gel was obtained after 1 h.

Chiral Memory Effect. The chiral BTECM gels containing chiral solvents *R*/*S*-terpinen-4-ol were casted on the quartz plates. After that, the quartz plates with BTECM gels were dried in the high vacuum for 24 h in order to completely remove the chiral solvents *R*/*S*-terpinen-4-ol. After vacuum-drying, the quartz plates with BTECM xerogels were measured using the CD spectrophotometer.

ASSOCIATED CONTENT

Supporting Information

The Supporting Information is available free of charge on the ACS Publications website at DOI: 10.1021/jacs.5b10496.

Synthetic procedures; Figures S1−S12 (PDF)

AUTHOR INFORMATION

Corresponding Authors

*E-mail twang@iccas.ac.cn (T.W.).
*E-mail liumh@iccas.ac.cn (M.L.).

Notes

The authors declare no competing financial interest.

ACKNOWLEDGMENTS

This work was supported by the Basic Research Development Program (2013CB834504), the National Natural Science Foundation of China (Nos. 91427302, 21227802, 21321063, and 21474118), "Strategic Priority Research Program" of the Chinese Academy of Sciences (XDB12020200), and the Fund of the Chinese Academy of Sciences.

REFERENCES

(1) (a) Bonner, W. *Origins Life Evol. Biospheres* **1995**, *25*, 175−190. (b) Feringa, B. L.; van Delden, R. A. *Angew. Chem., Int. Ed.* **1999**, *38*, 3418−3438.

(2) (a) Kondepudi, D. K.; Bullock, K. L.; Digits, J. A.; Hall, J. K.; Miller, J. M. *J. Am. Chem. Soc.* **1993**, *115*, 10211−10216. (b) Kondepudi, D. K.; Laudadio, J.; Asakura, K. *J. Am. Chem. Soc.* **1999**, *121*, 1448−1451. (c) Sakamoto, M.; Utsumi, N.; Ando, M.; Saeki, M.; Mino, T.; Fujita, T.; Katoh, A.; Nishio, T.; Kashima, C. *Angew. Chem., Int. Ed.* **2003**, *42*, 4360−4363. (d) Wu, S.-T.; Wu, Y.-R.; Kang, Q.-Q.; Zhang, H.; Long, L.-S.; Zheng, Z.; Huang, R.-B.; Zheng, L.-S. *Angew. Chem., Int. Ed.* **2007**, *46*, 8475−8479. (e) Noorduin, W. L.; Meekes, H.; van Enckevort, W. J. P.; Kaptein, B.; Kellogg, R. M.; Vlieg, E. *Angew. Chem., Int. Ed.* **2010**, *49*, 2539−2541. (f) Bisht, K. K.; Suresh, E. *J. Am. Chem. Soc.* **2013**, *135*, 15690−15693.

(3) (a) Link, D. R.; Natale, G.; Shao, R.; Maclennan, J. E.; Clark, N. A.; Körblova, E.; Walba, D. M. *Science* **1997**, *278*, 1924−1927. (b) Kajitani, T.; Kohmoto, S.; Yamamoto, M.; Kishikawa, K. *Chem. Mater.* **2005**, *17*, 3812−3819. (c) Jeong, K. U.; Yang, D. K.; Graham, M. J.; Tu, Y. F.; Kuo, S. W.; Knapp, B. S.; Harris, F. W.; Cheng, S. Z. D. *Adv. Mater.* **2006**, *18*, 3229−3232. (d) Choi, S.-W.; Izumi, T.; Hoshino, Y.; Takanishi, Y.; Ishikawa, K.; Watanabe, J.; Takezoe, H. *Angew. Chem., Int. Ed.* **2006**, *45*, 1382−1385. (e) Walba, D. M.; Korblova, E.; Huang, C. C.; Shao, R. F.; Nakata, M.; Clark, N. A. *J. Am. Chem. Soc.* **2006**, *128*, 5318−5319. (f) Hough, L. E.; Spannuth, M.; Nakata, M.; Coleman, D. A.; Jones, C. D.; Dantlgraber, G.; Tschierske, C.; Watanabe, J.; Körblova, E.; Walba, D. M.; Maclennan, J. E.; Glaser,

DOI: 10.1021/jacs.5b10496
J. Am. Chem. Soc. 2015, 137, 16109−16115

M. A.; Clark, N. A. *Science* **2009**, *325*, 452−456. (g) Nagayama, H.; Varshney, S. K.; Goto, M.; Araoka, F.; Ishikawa, K.; Prasad, V.; Takezoe, H. *Angew. Chem., Int. Ed.* **2010**, *49*, 445−448. (h) Ueda, T.; Masuko, S.; Araoka, F.; Ishikawa, K.; Takezoe, H. *Angew. Chem., Int. Ed.* **2013**, *52*, 6863−6866. (i) Dressel, C.; Liu, F.; Prehm, M.; Zeng, X.; Ungar, G.; Tschierske, C. *Angew. Chem., Int. Ed.* **2014**, *53*, 13115−13120.

(4) (a) DeRossi, U.; Daehne, S.; Meskers, S. C. J.; Dekkers, H. *Angew. Chem., Int. Ed. Engl.* **1996**, *35*, 760−763. (b) Ribó, J. M.; Crusats, J.; Sagués, F.; Claret, J.; Rubires, R. *Science* **2001**, *292*, 2063−2066. (c) Escudero, C.; Crusats, J.; Díez-Pérez, I.; El-Hachemi, Z.; Ribó, J. M. *Angew. Chem., Int. Ed.* **2006**, *45*, 8032−8035. (d) Spada, G. P. *Angew. Chem., Int. Ed.* **2008**, *47*, 636−638. (e) Crusats, J.; El-Hachemi, Z.; Ribó, J. M. *Chem. Soc. Rev.* **2010**, *39*, 569−577. (f) D'Urso, A.; Randazzo, R.; Lo Faro, L.; Purrello, R. *Angew. Chem., Int. Ed.* **2010**, *49*, 108−112. (g) Azeroual, S.; Surprenant, J.; Lazzara, T. D.; Kocun, M.; Tao, Y.; Cuccia, L. A.; Lehn, J.-M. *Chem. Commun.* **2012**, *48*, 2292−2294. (h) Micali, N.; Engelkamp, H.; van Rhee, P. G.; Christianen, P. C. M.; Scolaro, L. M.; Maan, J. C. *Nat. Chem.* **2012**, *4*, 201−207. (i) Stals, P. J. M.; Korevaar, P. A.; Gillissen, M. A. J.; de Greef, T. F. A.; Fitie, C. F. C.; Sijbesma, R. P.; Palmans, A. R. A.; Meijer, E. W. *Angew. Chem., Int. Ed.* **2012**, *51*, 11297−11301. (j) Sorrenti, A.; El-Hachemi, Z.; Arteaga, O.; Canillas, A.; Crusats, J.; Ribó, J. M. *Chem. - Eur. J.* **2012**, *18*, 8820−8826. (k) Romeo, A.; Castriciano, M. A.; Occhiuto, I.; Zagami, R.; Pasternack, R. F.; Scolaro, L. M. *J. Am. Chem. Soc.* **2014**, *136*, 40−43. (l) Liu, M.; Zhang, L.; Wang, T. *Chem. Rev.* **2015**, *115*, 7304−7397.

(5) (a) Zhang, S.; Yang, S.; Lan, J.; Yang, S.; You, J. *Chem. Commun.* **2008**, 6170−6172. (b) Kimura, M.; Hatanaka, T.; Nomoto, H.; Takizawa, J.; Fukawa, T.; Tatewaki, Y.; Shirai, H. *Chem. Mater.* **2010**, *22*, 5732−5738. (c) Shen, Z.; Wang, T.; Liu, M. *Angew. Chem., Int. Ed.* **2014**, *53*, 13424−13428. (d) Shen, Z.; Wang, T.; Shi, L.; Tang, Z.; Liu, M. *Chem. Sci.* **2015**, *6*, 4267−4272.

(6) Qiu, Y. F.; Chen, P. L.; Liu, M. H. *J. Am. Chem. Soc.* **2010**, *132*, 9644−9652.

(7) (a) Yuan, J.; Liu, M. *J. Am. Chem. Soc.* **2003**, *125*, 5051−5056. (b) Zhang, L.; Yuan, J.; Liu, M. *J. Phys. Chem. B* **2003**, *107*, 12768−12773. (c) Huang, X.; Li, C.; Jiang, S.; Wang, X.; Zhang, B.; Liu, M. *J. Am. Chem. Soc.* **2004**, *126*, 1322−1323. (d) Guo, P.; Zhang, L.; Liu, M. *Adv. Mater.* **2006**, *18*, 177−180. (e) Zhang, Y. Q.; Chen, P. L.; Liu, M. H. *Chem. - Eur. J.* **2008**, *14*, 1793−1803. (f) Zhang, Y. Q.; Chen, P. L.; Jiang, L.; Hu, W. P.; Liu, M. H. *J. Am. Chem. Soc.* **2009**, *131*, 2756−2757.

(8) (a) Tsuda, A.; Alam, M. A.; Harada, T.; Yamaguchi, T.; Ishii, N.; Aida, T. *Angew. Chem., Int. Ed.* **2007**, *46*, 8198−8202. (b) Okano, K.; Taguchi, M.; Fujiki, M.; Yamashita, T. *Angew. Chem., Int. Ed.* **2011**, *50*, 12474−12477.

(9) Helmich, F.; Smulders, M. M. J.; Lee, C. C.; Schenning, A. P. H. J.; Meijer, E. W. *J. Am. Chem. Soc.* **2011**, *133*, 12238−12246.

(10) Di Maria, F.; Olivelli, P.; Gazzano, M.; Zanelli, A.; Biasiucci, M.; Gigli, G.; Gentili, D.; D'Angelo, P.; Cavallini, M.; Barbarella, G. *J. Am. Chem. Soc.* **2011**, *133*, 8654−8661.

(11) (a) Würthner, F.; Kaiser, T. E.; Saha-Moller, C. R. *Angew. Chem., Int. Ed.* **2011**, *50*, 3376−3410. (c) Tanaka, M.; Ikeda, T.; Mack, J.; Kobayashi, N.; Haino, T. *J. Org. Chem.* **2011**, *76*, 5082−5091.

(12) (a) Sivadas, A. P.; Kumar, N. S.; Prabhu, D. D.; Varghese, S.; Prasad, S. K.; Rao, D. S.; Das, S. *J. Am. Chem. Soc.* **2014**, *136*, 5416−5423. (b) Cao, X.; Meng, L.; Li, Z.; Mao, Y.; Lan, H.; Chen, L.; Fan, Y.; Yi, T. *Langmuir* **2014**, *30*, 11753−11760.

(13) (a) Shirakawa, M.; Fujita, N.; Tani, T.; Kaneko, K.; Shinkai, S. *Chem. Commun.* **2005**, 4149−4151. (b) Kishimura, A.; Yamashita, T.; Aida, T. *J. Am. Chem. Soc.* **2005**, *127*, 179−183.

(14) (a) Bose, P. P.; Drew, M. G. B.; Das, A. K.; Banerjee, A. *Chem. Commun.* **2006**, *0*, 3196−3198. (b) López, J. L.; Atienza, C.; Seitz, W.; Guldi, D. M.; Martín, N. *Angew. Chem., Int. Ed.* **2010**, *49*, 9876−9880.

(15) Frisch, M. J.; Trucks, G. W.; Schlegel, H. B.; Scuseria, G. E.; Robb, M. A.; Cheeseman, J. R.; Scalmani, G.; Barone, V.; Mennucci, B.; Petersson, G. A.; Nakatsuji, H.; Caricato, M.; Li, X.; Hratchian, H. P.; Izmaylov, A. F.; Bloino, J.; Zheng, G.; Sonnenberg, J. L.; Hada, M.; Ehara, M.; Toyota, K.; Fukuda, R.; Hasegawa, J.; Ishida, M.; Nakajima, T.; Honda, Y.; Kitao, O.; Nakai, H.; Vreven, T.; Montgomery, J. A., Jr.; Peralta, J. E.; Ogliaro, F.; Bearpark, M.; Heyd, J. J.; Brothers, E.; Kudin, K. N.; Staroverov, V. N.; Kobayashi, R.; Normand, J.; Raghavachari, K.; Rendell, A.; Burant, J. C.; Iyengar, S. S.; Tomasi, J.; Cossi, M.; Rega, N.; Millam, J. M.; Klene, M.; Knox, J. E.; Cross, J. B.; Bakken, V.; Adamo, C.; Jaramillo, J.; Gomperts, R.; Stratmann, R. E.; Yazyev, O.; Austin, A. J.; Cammi, R.; Pomelli, C.; Ochterski, J. W.; Martin, R. L.; Morokuma, K.; Zakrzewski, V. G.; Voth, G. A.; Salvador, P.; Dannenberg, J. J.; Dapprich, S.; Daniels, A. D.; Farkas, Ö.; Foresman, J. B.; Ortiz, J. V.; Cioslowski, J.; Fox, D. J. *Gaussian 09, Revision D.01*; Gaussian, Inc.: Wallingford, CT, 2009.

(16) Martínez, L.; Andrade, R.; Birgin, E. G.; Martínez, J. M. *J. Comput. Chem.* **2009**, *30*, 2157−2164.

(17) Hess, B.; Kutzner, C.; van der Spoel, D.; Lindahl, E. *J. Chem. Theory Comput.* **2008**, *4*, 435−447.

(18) (a) Wang, J.; Wolf, R. M.; Caldwell, J. W.; Kollman, P. A.; Case, D. A. *J. Comput. Chem.* **2004**, *25*, 1157−1174. (b) Wang, J.; Wang, W.; Kollman, P. A.; Case, D. A. *J. Mol. Graphics Modell.* **2006**, *25*, 247−260.

(19) (a) Nakashima, H.; Koe, J. R.; Torimitsu, K.; Fujiki, M. *J. Am. Chem. Soc.* **2001**, *123*, 4847−4848. (b) Michinobu, T.; Shinoda, S.; Nakanishi, T.; Hill, J. P.; Fujii, K.; Player, T. N.; Tsukube, H.; Ariga, K. *J. Am. Chem. Soc.* **2006**, *128*, 14478−14479. (c) Katsonis, N.; Xu, H.; Haak, R. M.; Kudernac, T.; Tomovic, Z.; George, S.; Van der Auweraer, M.; Schenning, A.; Meijer, E. W.; Feringa, B. L.; De Feyter, S. *Angew. Chem., Int. Ed.* **2008**, *47*, 4997−5001. (d) Isare, B.; Linares, M.; Zargarian, L.; Fermandjian, S.; Miura, M.; Motohashi, S.; Vanthuyne, N.; Lazzaroni, R.; Bouteiller, L. *Chem. - Eur. J.* **2010**, *16*, 173−177. (e) George, S. J.; Tomovic, Z.; Schenning, A.; Meijer, E. W. *Chem. Commun.* **2011**, *47*, 3451−3453. (f) Chen, S.-G.; Yu, Y.; Zhao, X.; Ma, Y.; Jiang, X.-K.; Li, Z.-T. *J. Am. Chem. Soc.* **2011**, *133*, 11124−11127. (g) Nakano, Y.; Ichiyanagi, F.; Naito, M.; Yang, Y.; Fujiki, M. *Chem. Commun.* **2012**, *48*, 6636−6638. (h) Destoop, I.; Ghijsens, E.; Katayama, K.; Tahara, K.; Mali, K. S.; Tobe, Y.; De Feyter, S. *J. Am. Chem. Soc.* **2012**, *134*, 19568−19571.

(20) (a) Yashima, E.; Maeda, K.; Okamoto, Y. *Nature* **1999**, *399*, 449−451. (b) Lauceri, R.; Raudino, A.; Scolaro, L. M.; Micali, N.; Purrello, R. *J. Am. Chem. Soc.* **2002**, *124*, 894−895. (c) Ishi-i, T.; Crego-Calama, M.; Timmerman, P.; Reinhoudt, D. N.; Shinkai, S. *J. Am. Chem. Soc.* **2002**, *124*, 14631−14641. (d) Onouchi, H.; Miyagawa, T.; Morino, K.; Yashima, E. *Angew. Chem., Int. Ed.* **2006**, *45*, 2381−2384. (e) Mammana, A.; D'Urso, A.; Lauceri, R.; Purrello, R. *J. Am. Chem. Soc.* **2007**, *129*, 8062−8063. (f) Lauceri, R.; Fasciglione, G. F.; D'Urso, A.; Marini, S.; Purrello, R.; Coletta, M. *J. Am. Chem. Soc.* **2008**, *130*, 10476−10477. (g) George, S. J.; de Bruijn, R.; Tomovic, Z.; Van Averbeke, B.; Beljonne, D.; Lazzaroni, R.; Schenning, A. P.; Meijer, E. W. *J. Am. Chem. Soc.* **2012**, *134*, 17789−17796. (h) Helmich, F.; Lee, C. C.; Schenning, A.; Meijer, E. W. *J. Am. Chem. Soc.* **2010**, *132*, 16753−16755. (i) Zhang, W.; Jin, W.; Fukushima, T.; Ishii, N.; Aida, T. *J. Am. Chem. Soc.* **2013**, *135*, 114−117. (j) Castilla, A. M.; Ousaka, N.; Bilbeisi, R. A.; Valeri, E.; Ronson, T. K.; Nitschke, J. R. *J. Am. Chem. Soc.* **2013**, *135*, 17999−18006. (k) Nakashima, T.; Kobayashi, Y.; Kawai, T. *J. Am. Chem. Soc.* **2009**, *131*, 10342−10343.

DOI: 10.1021/jacs.5b10496
J. Am. Chem. Soc. 2015, 137, 16109−16115